Proceedings of the Combustion Institute, Volume 28, 2000/pp. 2793–2801

MECHANISMS OF CONCURRENT-FLOW FLAME SPREAD OVER SOLID FUEL BEDS

LINTON K. HONDA AND PAUL D. RONNEY
Department of Aerospace and Mechanical Engineering
University of Southern California
Los Angeles, CA 90089-1453, USA

It is proposed that concurrent-flow flame spread over solid fuel beds will be steady under conditions where heat and momentum losses to the sides of the fuel samples and/or surface radiative losses are significant. These losses are argued to be unavoidable because the flame length will grow until these losses balance the heat and momentum generation rates. Approximate relations (with no adjustable parameters or necessity for supplemental measured quantities such as heat fluxes or pyrolysis times) are derived for steady spread rates in the presence of these losses for laminar and turbulent flow, buoyant and forced convection, and thin and thick fuels. Experimental tests of these relations were conducted for upward flame spread over thermally thin fuels. Varying pressures, oxygen mole fractions, and diluents were employed to cover a seven-decade range of the Grashof number. These experiments generally support the validity of the proposed mechanisms.

Introduction

Flame spread over solid fuels is characterized as opposed-flow, where flames propagate opposite convection (corresponding to downward flame spread when buoyant convection dominates forced convection), or concurrent-flow (corresponding to upward spread.) Opposed-flow spread is reasonably well understood [1–4] since the spread rate (S_f) is typically steady due to balances between upstream diffusion and downstream convection of thermal energy. In contrast, for concurrent-flow spread, convective and diffusive transport are in the same direction, thus the fuel surface area exposed to high-temperature combustion products increases with time, leading to accelerating spread [2,3]. Consequently, concurrent-flow flame spread theory is less developed but has great practical importance to upward flame spread in building fires.

Using boundary-layer analyses, Fernandez-Pello [3] predicted that flame length (L) and S_f for concurrent flow ($S_{f,con}$) increase indefinitely with time (t) (Table 1). Delichatsios and collaborators [5] also examined unsteady concurrent-flow spread. In contrast, some experiments using thermally thin [6,7] and thermally thick [3,8,9] fuels show steady L and $S_{f,con}$. The analyses assumed adiabatic spread across infinitely wide samples, thus heat losses and lateral momentum losses were neglected. With such losses, the boundary layer thickness (δ) could not grow substantially larger than the sample width (W)—one could not expect 10 cm thick boundary layers on 1 cm wide fuel samples. If δ is limited, then L and S_f are also limited. Even for infinitely wide samples, L could not grow indefinitely because surface radiative losses would eventually exceed heat generation rates. Both assertions arise because for boundary-layer flows, the fuel-bed heat flux (Q), thus fuel vapor generation rates and total heat generation rates, increase more weakly than linearly with L, whereas heat and lateral momentum losses increase roughly linearly with L. (Markstein and deRis [10] suggested that for thermally thin beds, fuel burnout could limit S_f, but not for practical sample dimensions.) Hence, we propose the following:

1. For sufficiently narrow fuel beds, L grows until $\delta \approx W$, when transverse heat and momentum losses prevent further growth of L, which limits Q and thus S_f.
2. For sufficiently wide fuel beds, L grows until surface radiative loss is comparable to Q, when these losses prevent further growth of L, which limits Q and thus S_f.

TABLE 1
Predicted variation in spread rate ($S_{f,con}$) and flame length (L) with time (t) for laminar concurrent-flow flame spread

Fuel Type	Buoyant Convection	Forced Convection
Thermally thin	$S_{f,con} \sim t^3, L \sim t^4$	$S_{f,con} \sim t^1, L \sim t^2$
Thermally thick	$S_{f,con} \sim t^1, L \sim t^2$	$S_{f,con} \sim t^0, L \sim t^1$

Note: From Ref. [3] and references therein.

TABLE 2
Predicted relations for the steady values of Nu_L and L/W for forced or buoyant convection and convective or surface radiation

Stabilization Type	Buoyant Convection		Forced Convection	
	Nu_L	L/W	Nu_L	L/W
Convective	$DC^{-3d/1-3c}\,Gr_W^{d/1-3c}$	$C^{-1/1-3c}\,Gr_W^{c/1-3c}$	$BA^{-b/1-a}\,\mathrm{Re}_W^{b/1-a}$	$A^{-1/1-a}\,\mathrm{Re}_W^{a/1-a}$
Radiative	$D^{1/1-3d}\,Pl_W^{3d/1-3d}\,Gr_W^{d/1-3d}$	$D^{1/1-3d}\,Pl_W^{1/1-3d}\,Gr_W^{d/1-3d}$	$B^{1/1-a}\,Pl_W^{b/1-a}\,\mathrm{Re}_W^{b/1-a}$	$B^{1/1-b}\,Pl_W^{1/1-b}\,\mathrm{Re}_W^{b/1-b}$

Note: Predictions are the same for thermally-thin and thermally-thick fuels. Since $Re_w \sim W$, $Gr_w \sim W^3$ and $Pl_w \sim W^{-1}$, L is independent of W for radiatively stabilized flames.

We designate these flames as *convectively stabilized* and *radiatively stabilized.* Although heat and momentum losses are considered, no finite-rate chemistry effects are considered; consequently, these hypotheses apply only *far from extinction conditions.*

Note that we treat radiative loss simply as a surface loss with no gas-phase reabsorption. Our estimates indicate this approximation is reasonable since solid fuels emit as roughly gray bodies whereas gases absorb only in narrow spectra bands. Optically-thin gas-phase radiation was considered as another loss mechanism but rejected because it is isotropic, hence the loss is balanced by increased radiative flux to the fuel bed, yielding little net effect on S_f. Gas-phase radiation affects the mass burning rate of fully developed fires on thick vertical walls, but we are analyzing only S_f for developing fires.

In this work, simple models of loss-limited concurrent-flow flame spread have been developed based on these hypotheses. Experiments were conducted to test the resulting predictions. We emphasize that there are no adjustable parameters nor necessity for supplemental empirical quantities such as surface heat fluxes [9,10] or pyrolysis times [5].

Modeling Predictions

Flame Lengths

Boundary-layer analyses are appropriate for concurrent-flow flame-spread analyses [2,3]; thus for forced-convection flame spread, we assumed $\delta = LARe_L^{-a}$ and $Nu_L = BRe_L^b$ (A, B, a, and b are constant), where Nu_L is the length-averaged Nusselt number, $Re_L \equiv UL/\nu_g$ is the Reynolds number, U is the forced convection velocity, and ν_g is the kinematic viscosity. For buoyant-convection-dominated spread, we assumed $\delta = LCGr_L^{-c}$ and $Nu_L = DGr_L^d$, where $Gr_L \equiv gL^3/\nu_g^2$ is the Grashof number. We assumed Prandtl numbers (Pr) close to unity and that the thermal expansion term generally present in Gr_L is close to unity, which is reasonable since the product density is 5–8 times smaller than the reactant density. For laminar flow, classical models yield (based on the momentum boundary layer thickness, for $Pr = 0.72$) $A = 0.664$, $a = 1/2$, $B = 0.595$, $b = 1/2$ [11], and (defining δ as the horizontal distance from the fuel surface to the location of the velocity maximum) $C = 1.37$, $c = 1/4$, $D = 0.476$, and d

TABLE 3
Predicted relations for steady values of $S_{f,con}/S_{f,opp}$ for thin and thick fuels, forced and buoyant convection, and convective and surface radiative loss stabilization

Stabilization Type/Fuel Type	Buoyant Convection	Forced Convection
Convective/thin	$\frac{4}{\pi} DC^{-3d/1-3c}\, Gr_W^{d/1-3c}$	$\frac{4}{\pi} BA^{-b/1-a}\, Re_W^{b/1-a}$
Radiative/thin	$\frac{4}{\pi} D^{1/1-3d}\, Pl_W^{3d/1-3d}\, Gr_W^{d/1-3d}$	$\frac{4}{\pi} B^{1/1-b}\, Pl_W^{b/1-b}\, Re_W^{b/1-b}$
Convective/thick	$\frac{D^2}{E} C^{1-6d/1-3c}\, Gr_W^{-(1\,-\,6d)/3(1\,-\,3c)}$	$B^2 A^{1-2b/1-a}\, Re_W^{-(1-2b)/1-a}$
Radiative/thick	$\frac{D^{1/1-3d}}{E} Pl_W^{-(1-6d)/1-3d}\, Gr_W^{-(1-6d)/3(1-3d)}$	$B^{1/1-b}\, Pl_W^{-(1-2b)/1-b}\, Re_W^{-(1-2b)/1-b}$

Note: Since $Re_w \sim W$, $Gr_w \sim W^3$, and $Pl_w \sim W^{-1}$, $S_{f,con}$ is always independent of W for radiatively stabilized flames.

$= 1/4$ [12]. For turbulent flow, $A = 0.14$, $a = 1/7$, $B = 0.0131$, and $b = 6/7$ [13], and (at $Gr_L < 10^{10}$, corresponding to all conditions we could study), $C = 0.030$, $c = 0.10$ [14,15], $D = 0.474$, and $d = 0.25$ [16].

Hypothesis 1 states $\delta \approx W$, consequently

$$L/W \approx A^{-1/1-a}\, Re_W^{a/1-a}$$

$$Nu_L \approx BA^{-b/1-a}\, Re_W^{b/1-a}$$

$$Re_W \equiv \frac{UW}{v_g} \text{ (forced convection)} \tag{1a}$$

$$L/W \approx C^{-1/1-3c}\, Gr_W^{c/1-3c}$$

$$Nu_L \approx DC^{-3d/1-3c}\, Gr_W^{d/1-3c}$$

$$Gr_W \equiv \frac{gW^3}{v_g^2} \text{ (buoyant convection)} \tag{1b}$$

where all gas properties are temperature averaged as discussed later. Note that L/W and Nu_L are expressed through known experimental conditions Re_w or Gr_w rather than unknown Re_L or Gr_L.

Hypothesis 2 states that $Q = (Nu_L\lambda_g/L)(T_f - T_v)$ equals the radiative loss from the bed $(H) = \sigma\varepsilon(T_v^4 - T_\infty^4)$, where λ_g, σ, ε, T_f, T_v, and T_∞, are the gas thermal conductivity, Stefan-Boltzman constant, bed emissivity, flame temperature [1], vaporization temperature, and ambient temperature, respectively. Thus

$$L/W \approx B^{1/1-b}\, Pl_W^{1/1-b}\, Re_W^{b/1-b}$$

$$Nu_L \approx B^{1/1-b}\, Pl_W^{b/1-b}\, Re_W^{b/1-b}$$

$$\text{(forced convection)} \tag{2a}$$

$$L/W \approx D^{1/1-3d}\, Pl_W^{1/1-3d}\, Gr_W^{d/1-3d}$$

$$Nu_L \approx D^{1/1-3d}\, Pl_W^{3d/1-3d}\, Gr_W^{d/1-3d}$$

$$\text{(buoyant convection)} \tag{2b}$$

where $Pl_W \equiv \lambda_g(T_f - T_v)/W\varepsilon\sigma(T_v^4 - T_\infty^4)$ is the Planck number. Equations 1 and 2 then yield predictions for L/W and Nu_L (Table 2).

Spread Rates

$S_{f,con}$ is estimated by equating Q to the rate of fuel-bed enthalpy increase $(= \rho_s C_{p,s}\tau_s(T_v - T_\infty)WS_f$, where ρ_s, $C_{p,s}$, and τ_s are the fuel-bed density, heat capacity, and thickness, respectively). Thus, for thermally thin fuels,

$$S_{f,con}/S_{f,opp} = \frac{4}{\pi}\, Nu_L$$

$$S_{f,opp} = \frac{\pi}{4}\,\frac{\lambda_g}{\rho_s C_{p,s}\tau_s}\left(\frac{T_f - T_v}{T_v - T_\infty}\right) \tag{3}$$

where for compactness $S_{f,con}$ is referenced to S_f for laminar, opposed-flow spread $(S_{f,opp})$ [17].

For thick fuels, $S_{f,con}$ is estimated by substituting the solid thermal penetration depth (τ_p) [1] for τ_s in equation 3, τ_p is estimated by equating Q to the heat flux from the fuel surface into the bed $= \lambda_s(T_v - T_\infty)/\tau_p$, where λ_s is the solid thermal conductivity. This yields

$$\tau_p = \frac{L}{Nu_L}\,\frac{\lambda_s}{\lambda_g}\,\frac{T_v - T_\infty}{T_f - T_v} \tag{4}$$

With $\tau_p = \tau_s$, equations 3 and 4 yield

$$S_{f,con}/S_{f,opp} = Nu_L^2\left(\frac{L}{W}\right)^{-1}\left(\frac{U_{opp}W}{v_g}\right)^{-1}$$

$$S_{f,opp} = U_{opp}\,\frac{\rho_g C_{p,g}\lambda_g}{\rho_s C_{p,s}\lambda_s}\left(\frac{T_f - T_v}{T_v - T_\infty}\right)^2 \tag{5}$$

Combining equations 3–5 with Nu_L from Table 2 yields predictions for $S_{f,con}$ (Table 3). For forced flow, $U_{opp} = U$ is prescribed. Whereas for buoyant flow, U_{opp} cannot be prescribed; we employ the estimate $U_{opp} \approx E^{1/3}(gv_g)^{1/3}$, where $E \approx (0.72/Pr)(T_f - T_v)/T_\infty$ [1]. This estimate of U_{opp} for buoyant flow is incorporated into thick-fuel predictions (Table 3).

This analysis is readily extended to unsteady spread by neglecting loss mechanisms and setting $S_f = dL/dt$ rather than $S_f =$ constant. This leads to first-order differential equations for $L(t)$. For example, for thin fuels under buoyant flow,

$$S_{f,con}(t) \approx \frac{dL}{dt} \approx \frac{4}{\pi} Nu_L(t) S_{f,opp} \approx \frac{4C}{\pi} Gr_L(t)^c$$

$$= \frac{4C}{\pi} Gr_W^c \left(\frac{L(t)}{W}\right)^{3c} S_{f,opp} \tag{6a}$$

which has the solution

$$S_{f,con} = \frac{1}{1 - 3c}\left(\frac{4C(1 - 3c)}{\pi}\left(\frac{Gr_W}{W^3}\right)^c S_{f,opp}\right)^{1/1-3c} t^{3c/1-3c} \tag{6b}$$

For laminar flow ($c = 1/4$),

$$S_{f,con} = 4\left(\frac{C}{\pi}\right)^4 S_{f,opp}^4\,\frac{Gr_W}{W^3}\,t^3 \tag{6c}$$

which has the form $S_f \sim t^3$, proposed by Fernandez-Pello [3] (Table 1). The other relations in Table 1 can be derived similarly. Thus, our proposed approach is considered quite general.

Transitions between Regimes

Transition between laminar and turbulent flame spread occurs when Re_L or Gr_L exceeds critical values, denoted $Re_L^* \approx 5 \times 10^5$ and $Gr_L^* \approx 4 \times 10^8$. By writing $Re_W = Re_L/(L/W)$ and $Gr_W = Gr_L/(L/W)^3$, with expressions for L/W taken from Table 2,

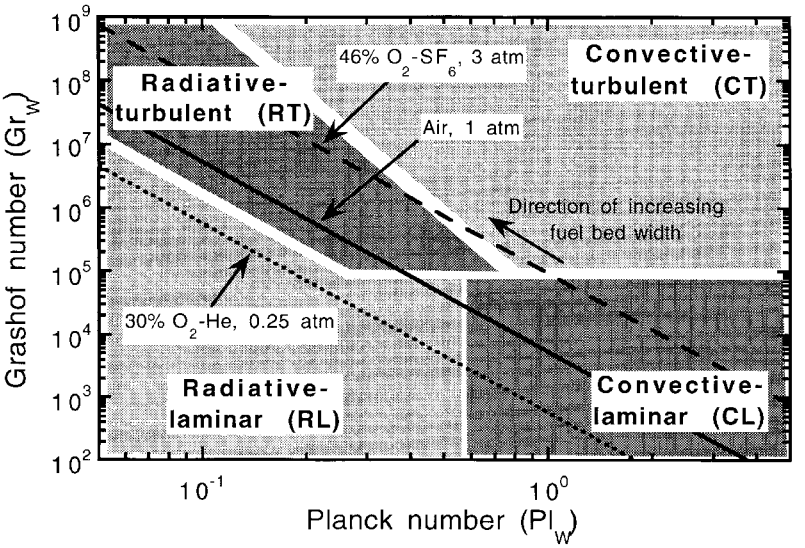

FIG. 1. Predicted regimes of concurrent-flow flame spread for buoyant convection, showing the type of flow (laminar or turbulent) and type of flame stabilization (convective or radiative). Also shown are lines corresponding to a fixed atmosphere but varying fuel bed width (W) for air, and the atmospheres yielding the lowest and highest Pl_W and Gr_W tested experimentally in this work, i.e., 0.25 atm O_2-He and 3 atm O_2-SF_6, respectively, for $T_v = 618$ K, $T_\infty = 300$ K, and $\varepsilon = 1$.

we infer at transition, for convectively stabilized flames

$$Re_W = A(Re_L^*)^{1-a} \text{ (forced)}$$

$$Gr_W = C^3(Gr_L^*)^{1-3c} \text{ (buoyant)} \quad (7a)$$

and for radiatively stabilized flames

$$Re_W = B^{-1}(Re_L^*)^{1-b}\, Pl_W^{-1} \text{ (forced)}$$

$$Gr_W = D^{-3}(Gr_L^*)^{1-3d}\, Pl_W^{-3} \text{ (buoyant)} \quad (7b)$$

Transition between convective and radiative stabilization occurs when the predicted L are equal, thus

$$Pl_W = \frac{1}{B}\left(\frac{1}{A}\right)^{1-b/1-a} Re_W^{a-b/1-a} \text{ (forced)}$$

$$Pl_W = \frac{1}{D}\left(\frac{1}{C}\right)^{1-3d/1-3c} Gr_W^{c-d/1-3c} \text{ (buoyant)} \quad (8)$$

Figure 1 shows flame spread regimes for buoyant flow, obtained by mapping these transitions into (Gr_W, Pl_W) space and eliminating inconsistent transitions (for example direct transition from convective stabilization/laminar flow (CL) to radiative stabilization/turbulent flow (RT)). Figure 1 also shows combinations of Gr_W and Pl_W accessible by varying W for ambient air, 0.25 atm O_2-He, and 3 atm O_2-SF_6 atmospheres, the latter two having the highest and lowest v_g we employed. (In Fig. 1 and subsequent predictions, λ_g and v_g are taken as averages of values at T_∞ and T_f, assuming $\lambda_g \sim T^{0.75}$ and $v_g \sim T^{1.75}$.) For small W, CL spread always applies. For high-v_g atmospheres, only transition to radiative stabilization/laminar flow (RL) occurs. For lower v_g, transition to RT occurs, possibly with intermediate RL or CT regimes for marginal ranges of W.

Comparison with Previous Results

Relatively few experimental or computational results are available for comparison with these predictions. Thin-fuel buoyant-flow experiments at low pressure (P) ([6], Fig. 14) in 30%O_2/70%N_2 atmospheres with small W (10 mm) show $S_{f,con} \sim P^{1.8}$. This is close to our prediction $S_f \sim P^2$ for CL or RL spread (with $c = d = 1/4$, $S_f \sim Gr_W^1$ (CL) or $S_f \sim Gr_W^1 Pl_W^3$ (RL); since $Gr_W \sim v_g^{-2} \sim P^2$ and $Pl_W \sim \lambda_g^1 \sim P^0$, $S_f \sim P^2$). In contrast, for downward (opposed-flow) flame spread, $S_f \sim P^0$ [1,18]. Concurrent laminar forced-flow experiments [8,9] over wide, thermally thick polymethyl methacrylate (PMMA) sheets show $S_f \sim U^1$ behavior, consistent with Table 3 for thick CL or RL spread, since for $a = b = 1/2$, $S_{f,con} \sim Re_W^0$ $S_{f,opp} \sim U^1$. (In Ref. [9], grid turbulence was employed, but $Re_L < Re_L^*$ for all test conditions, plus turbulence intensity had little effect on S_f; thus laminar values of a and b apply). Adiabatic

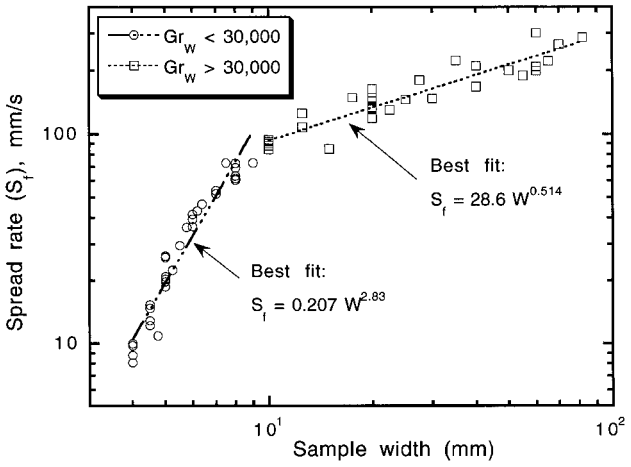

FIG. 2. Effect of fuel bed width (W) on upward flame spread rate ($S_{f,con}$) for thin fuel beds burning in ambient air. Predicted results are $S_f \sim W^3$ for low Gr_W and $S_f \sim W^0$ for high Gr_W, with a transition Gr_W of 30,000.

analyses (Table 1) also predict $S_{f,con} \sim U^1$, but predict $L \sim t^1$, whereas our non-adiabatic analysis predicts steady $L \sim Re_W^1$. Unfortunately, no time-dependent data on L were reported in Ref. [8,9] to compare adiabatic and non-adiabatic models. Ferkul and Tien [19] modeled concurrent forced-flow flame spread over two-dimensional (infinitely wide, thus convective stabilization cannot apply) thermally thin samples with surface radiative loss and predicted steady spread with $S_{f,con} \sim U^1$ (whereas $S_{f,opp} \sim U^0$ [1]) and $L \sim U^1$, consistent with Tables 2 and 3 for RL spread. In contrast, adiabatic analyses predict $S_{f,con} \sim t^1$ for these assumptions (Table 1). Jiang et al. [20] found $S_{f,con} \sim g^1$ and $L \sim g^1$ for concurrent buoyant spread, again consistent with RL predictions.

Experiments

Apparatus and Procedures

Although few data are available for comparison with Tables 2 and 3, these data are generally consistent with predictions. Comprehensive data sets were generated for thin fuels under buoyant convection by measuring the effects of W, P, τ_s, and diluent type on $S_{f,con}$. To obtain small Gr_w, small W and P were employed. These conditions cause flame quenching, hence elevated oxygen concentrations (at least 4 mol % above quenching limits) were used, enabling steady upward spread for Gr_w down to 3×10^2 in O_2-He atmospheres at low pressure (large v_g). To obtain large Gr_W, CO_2 and SF_6 diluents at high pressure (small v_g) with large W were employed. While large Gr_W results in large flame length, using a 2 m tall chamber enabled steady spread (defined as steady S_f *and* L) at Gr_W up to 3×10^9, corresponding to $W = 41$ cm in ambient air. (At still larger Gr_w, steady spread was not reached within the available distance; such data were discarded.) Consequently, a seven-decade range of Gr_W exhibiting steady spread could be examined. Steady spread was defined to be when the pyrolysis front and flame leading edge propagated at identical and steady rates with constant flame length (L). The necessary reference values of $S_{f,opp}$ were measured for downward propagation over samples sufficiently wide that $S_{f,opp}$ was independent of W.

The apparatus employed was similar to that used in prior studies [18] except for the taller chamber (2 m). The chamber gases were generated via the partial pressure method. Kimwipes fuel samples ($\rho_s\tau_s = 0.0018$ g/cm^2) of single or double thickness were held by aluminum clamps to inhibit edge burning and were ignited by electrically heated wires. Type-S thermocouples (50 μm diameter) having 50 ms typical response time were attached to the clamp. Thermocouple voltages were recorded by a PC-based data acquisition system. The flames were recorded on video, S_f was inferred from video records or thermocouple data; these were identical within experimental uncertainty. Estimated uncertainties in S_f, temperature, O_2 mole fraction, and total pressure were 5%, 5%, 1%, and 0.5%, respectively.

Results

Figure 2 shows the effect of W on $S_{f,con}$ for ambient air. At low Gr_W, $S_{f,con} \sim W^{2.83}$, thus $S_{f,con}/S_{f,opp} \sim Gr_W^{0.94}$, close to the CL prediction (Table 3) $S_{f,con}/S_{f,opp} \sim Gr_W^1$. At $Gr_W > 30{,}000$, $S_{f,con} \sim W^{0.51}$, thus $S_{f,con}/S_{f,opp} \sim Gr_W^{0.17}$, close to RL or RT predictions since $S_{f,con}/S_{f,opp} \sim Gr_W^1 Pl_W^3 \sim W^3 W^{-3} \sim W^0$. The observed transition Gr_W is close to the CL-RL prediction $Gr_W \approx 30{,}000$ (Fig. 1). This should be followed by RL-RT transition at $Gr_W \approx 90{,}000$, but this cannot be discerned because the Gr_W range corresponding to RL behavior is narrow. Furthermore,

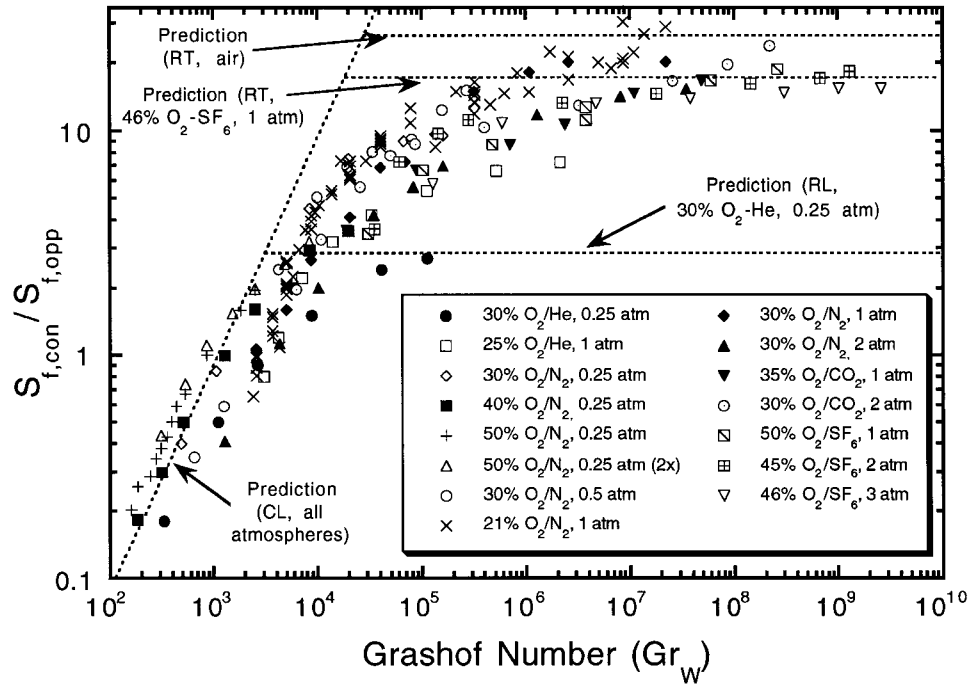

FIG. 3. Correlation of steady values of $S_{f,con}/S_{f,opp}$ with Gr_W for all experimental data. "2x" indicates double-thickness fuel samples.

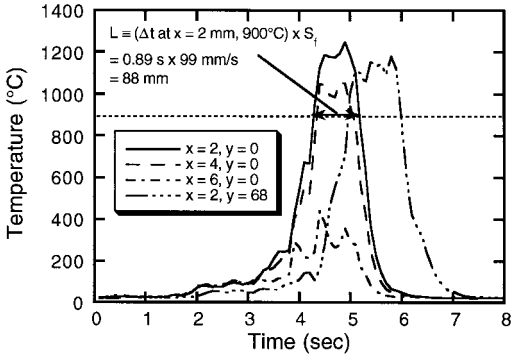

FIG. 4. Example of temperature versus time history for upward-spreading flame in air at 1 atm over a 10 mm wide fuel bed ($Gr_W = 4.5 \times 10^4$). "x" values denote horizontal distance from fuel surface in mm; "y" values denote vertical distance from primary measurement station in mm.

there is little difference between RL and RT predictions for S_f since D and d are only slightly different for laminar versus turbulent flow.

Figure 3 shows the correlation between $S_{f,con}/S_{f,opp}$ and Gr_W for all data. At low Gr_w, the proposed relation $S_{f,con}/S_{f,opp} \sim Gr_w^1$ fits each data set for a given atmosphere well, although between different atmospheres a factor of 2.5 variation in $S_{f,con}/S_{f,opp}$ is found at constant Gr_w. Nevertheless, the comparison is considered quite reasonable considering the wide range of experimental conditions tested. We believe much of the scatter resulted from varying degrees of dissociation for various atmospheres, which in turn affected temperature averaging. At higher Gr_w, all data bend toward the horizontal, indicating $S_{f,con}/S_{f,opp} \sim Gr_w^0$, consistent with radiative stabilization. The transition Gr_W varies from about 5000 for the highest v_g atmosphere tested (30% O_2-He, 0.25 atm) to 200,000 for the lowest v_g tested (46% O_2-SF_6, 3 atm). These transitions are in very good agreement with predictions (Fig. 1). $S_{f,con}/S_{f,opp}$ predictions are in very good agreement with experiments for high and intermediate v_g, though high for the lowest v_g (3 atm O_2-SF_6) predictions are slightly off the graph.

Figure 3 shows the utility of the proposed scalings; wide ranges of S_f and Gr_W for varying Pl_W are correlated on one plot. Effects of Lewis number [18] and other mixture properties are covered by referencing $S_{f,con}$ to $S_{f,opp}$. For convectively stabilized flames, T_f effects appear only through temperature-averaging of transport properties. T_v effects appear only for radiative-stabilized flames (through Pl_W).

Flame lengths were measured from thermocouple data (Fig. 4). Temperatures rise sharply then plateau upon flame leading edge arrival, then fall sharply upon trailing edge passage. Note that temperature

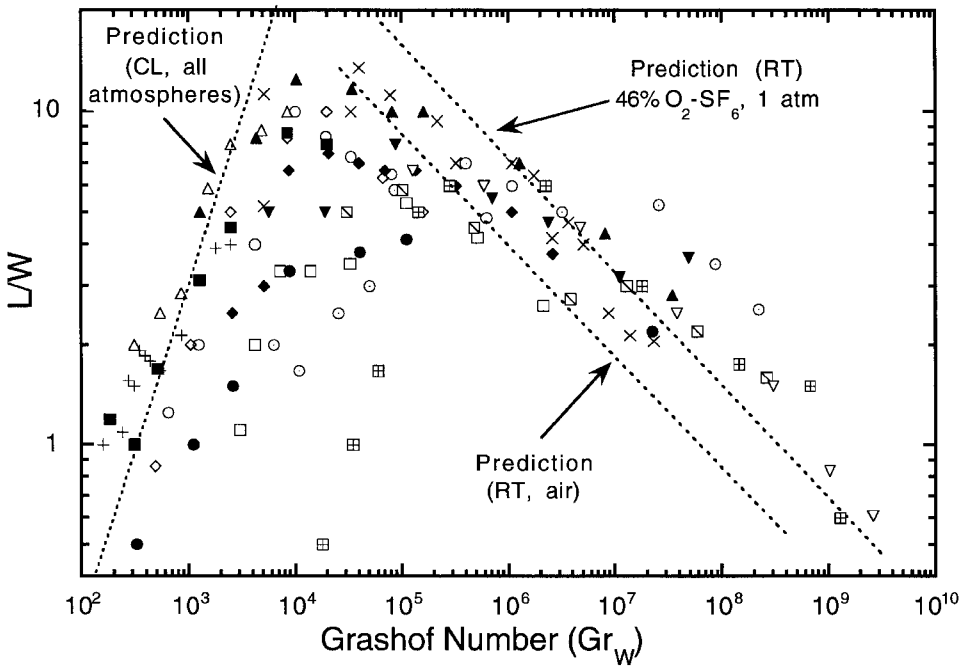

FIG. 5. Correlation of steady values of L/W with Gr_W for all experimental data. Legend is the same as for Fig. 3.

histories at two vertical locations ($y = 0$, $y = 68$) are very similar, indicating steady spread. L was defined as $S_f(\Delta t)$, where Δt is the time lapse between the leading and trailing edge passage at 900 °C, because this gave good agreement with visible flame lengths. (Thermocouple-based lengths were more consistent and thus preferred for quantitative measurement). The thermocouple closest to the surface (2 mm) was used because for small v_g, δ was very small, consequently, more remote thermocouples exhibited no significant temperature rise. Fig. 5 shows correlations of L/W with Gr_W. At low Gr_W, most data for a given atmosphere follow the predicted $L/W \sim Gr_W^1$ for CL spread (Table 2), albeit with substantial scatter between different atmospheres. For large W, $L/W \sim Gr_W^{-1/3}$, as required for width-independent L.

A critical aspect of our hypotheses is that S_f is determined by Nu_L, which in turn is determined by L. From Tables 2 and 3, the predicted relationships between $S_{f,con}$ and L for buoyant flow are

$$L/W \approx \frac{1}{C}\left(\frac{4}{\pi}D\right)^{-c/d}\left(\frac{S_{f,con}}{S_{f,opp}}\right)^{c/d}$$

(convective stabilization) (9a)

$$L/W \approx \left(\frac{4}{\pi}D\right)^{-1/3d} Gr_W^{-1/3}\left(\frac{S_{f,con}}{S_{f,opp}}\right)^{1/3d}$$

(radiative stabilization) (9b)

Fig. 6 shows the ratios of the left-hand to right-hand sides of these equations, based on measured $S_{f,con}/S_{f,opp}$ and L/W. For large Gr_W, agreement with RT predictions is very good; for $Gr_W > 200{,}000$, the mean ratio is 1.63 with a standard deviation of 37% of the mean. For smaller Gr_W, either CL or RT predictions are roughly consistent with experiments (though offset by factors of about 3), but only CL predictions are consistent with S_f data (Fig. 3), as predicted by Fig. 1. Fig. 1 suggests that atmospheres with the smallest v_g might exhibit CT behavior for marginal ranges of Gr_W; while no data in Fig. 6 are consistent with CT predictions, intermediate Gr_W (10^4–10^5) come closest, as expected based on Fig. 1. Consequently, the relationships between measured L and $S_{f,con}$ are generally consistent with our modeling hypotheses considering the transitions between regimes.

Conclusions

Models of concurrent-flow flame spread were developed, hypothesizing that for narrow fuel beds, lateral heat and/or momentum losses limit flame length, and for wide fuel beds, surface radiation losses limit flame length. These losses lead to steady rather than accelerating spread for sufficiently tall beds. Spread rate predictions were developed for thermally thin and thermally thick fuel beds. These results were generally in agreement with limited

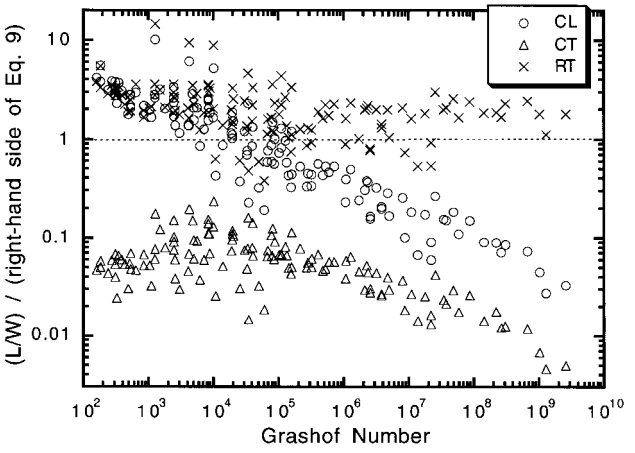

FIG. 6. Ratio of measured L/W to right-hand sides of equations 9a and 9b, showing comparison of predicted and observed correlation of L to $S_{f,con}$ for convective-laminar, convective-turbulent, and radiative-turbulent spread regimes (see Fig. 1). Dashed horizontal line indicates ideal fit of prediction to experiments.

prior experimental and theoretical results. Upward flame spread experiments were performed for thermally thin beds for varying width, thickness, pressure, and oxygen concentration. These data generally support the proposed models. The results may be useful in developing improved models of concurrent-flow flame spread in more complex geometries, such as upward fire spread in enclosures. In future work, thermally thick fuels will be studied, since these conditions are relevant to wall fires in buildings.

Acknowledgments

This work was supported by NASA-Glenn under grants NAG3-1611 and NCC3-671. We thank Drs. Michael Delichatsios and Suleyman Gokoglu for helpful discussions.

REFERENCES

1. deRis, J. N., *Proc. Combust. Inst.* 12:241–252 (1968).
2. Williams, F. A., *Proc. Combust. Inst.* 16:1281–1294 (1976).
3. Fernandez-Pello, A. C., *Combust. Sci. Technol.* 39:119–134 (1984).
4. Bhattacharjee, S., West, J., and Dockter, S., *Combust. Flame* 104:66–80 (1996).
5. Delicahatsios, M. A., Delichatsios, M., Chen, Y., and Hasemi, Y., *Combust. Flame* 102:357–370 (1995).
6. Fernandez-Pello, A. C., and Hirano, T., *Combust. Sci. Technol.* 32:1–31 (1983).
7. Grayson, G. D., Sacksteder, K. R., Ferkul, P., and T'ien, J. S., *Micrograv. Sci. Technol.* 7:187–195 (1994).
8. Loh, H. T., and Fernandez-Pello, A. C., *Proc. Combust. Inst.* 20:1575–1582 (1984).
9. Zhou, L., and Fernandez-Pello, A. C., *Combust. Flame* 92:45–59 (1993).
10. Markstein, G. H., and deRis, J., *Proc. Combust. Inst.* 12:1085–1097 (1972).
11. Schlichting, H., *Boundary Layer Theory, 4th ed.,* McGraw-Hill, New York, 1960.
12. Gebhart, B., Jaluria, Y., Mahajan, R. L., and Sammakia, B., *Buoyancy-Induced Flows and Transport,* Hemisphere, Washington, D.C., 1988.
13. White, F. M., *Viscous Fluid Flow,* McGraw-Hill, New York, 1974.
14. Mason, H. B., and Seban, R. A., *Int. J. Heat Mass Transfer* 17:1329–1336 (1974).
15. Cheesewright, R., *J. Heat Trans.* 90:1 (1968).
16. Churchill, S. W., and Usagi, R., *AIChE J.* 18:1121 (1972).
17. Delichatsios, M. A., *Combust. Sci. Technol.* 44:257–267 (1986).
18. Zhang, Y., Ronney, P. D., Roegner, E., and Greenberg, J. B., *Combust. Flame* 90:71–83 (1992).
19. Ferkul, P. V., and T'ien, J. S., *Combust. Sci. Technol.* 99:345–370 (1994).
20. Jiang, C.-B., T'ien, J. S., and Shih, H.-Y., *Proc. Combust. Inst.* 26:1353–1360 (1996).

COMMENTS

Michael Delichatsios, CSIRO, Australia. The main reason for steady flame spread in your upward flame-spread situation is that the material burns out (or chars out). This situation is represented by your experiments. The effects of width are to change the X/X_p (Flame length/pyrolysis length) ratio and the heat flux to the surface. Can you extrapolate the results for infinite width and discuss the interpretation? Roughly speaking the burnout length is $l_b = U_s t_b$ where U_s is spread velocity and t_b is burnout time.

Author's Reply. We agree that the fuel bed width affects the flame length and heat flux, as discussed in our presentation and paper. Our analysis and experiments support the conclusion these are controlled by heat losses from the flame and fuel surface in a way that is width-dependent for narrow samples, but width-independent for wide samples. The transition occurs due to a change in the dominant mechanism of loss. It is not clear to us how this transition would occur if burnout length were controlling the process. Moreover, we have recent results (not yet published) for thermally thick fuels that show that steady spread does occur in such cases with a rate dependent on the sample width, even though there is no burnout in this case.

•

John L. de Ris, Factory Mutual Research, USA. I would like to compliment the authors for such an impressive study into the mechanisms of upward fire spread. It would be interesting for the authors to comment on the early study of Phillip Thomas who developed the first model for upward spread. Also the authors might comment on the study by George Markstein and myself who found the flames continued to accelerate for very wide fuel widths.

Author's Reply. Thank you for bringing the paper by P. H. Thomas and C. T. Webster in *Fire Research Note 420,* 1960, to our attention. Their experiment was somewhat different than ours in that their samples were unclamped and curled as they burned. Their analysis is based on entrainment from a round jet rather than a boundary layer over a flat fuel surface. They did not report values of $S_{f,opp}$, but if we use a calculated value (based on equation 3) of 0.21 cm/s then their results can be compared to our Fig. 3. Their results are similar to ours but higher by a factor of about 2, which might be due to the difference in geometries.

Concerning the paper by Markstein and deRis [Ref. 10 in paper], with our 2 m tall apparatus we could only obtain steady upward spread in air for $W < 8$ cm. Our results apply only for sufficiently tall samples; if the sample is too short, steady spread will not be reached. Since L/W can be greater than 10 (Fig. 5), plus we found that the development length is several times the steady-state flame length, quite tall samples are needed to reach steady state over wide samples. This same conclusion was found [10], where only samples with $W > 15$ cm were tested, and a steady-state flame length of typically 2 m was predicted based on extrapolation of experimental data on samples of up to 1.5 m in length.